Proceedings of ASME Turbo Expo 2016: Turbine Technical Conference and Exposition
GT2016
June 13-17, 2016, Seoul, South Korea

GT2016-57490

ANALYSIS OF COMBUSTION NOISE USING LOCALLY RESOLVED DENSITY FLUCTUATIONS AND A MICROPHONE ARRAY

Johannes Peterleithner, Stefan Zerobin, Jakob Woisetschläger
Institute for Thermal Turbomachinery and Machine Dynamics, Graz University of Technology
8010 Graz, Austria

ABSTRACT

For turbulent swirl-stabilized flames combustion noise can be directly calculated, if density fluctuations as a function of time and space are known. It is however not easily possible to assess the density fluctuations directly. Therefore, in the past, combustion noise has been expressed as a function of chemiluminescence, an approach bringing in more assumptions. Now, by using interferometry, density fluctuations in the flame can be measured quantitatively. The advantage of this technique is that it measures the time derivative of density fluctuations directly. In this work laser interferometric vibrometry (LIV) was used to scan a two dimensional field in the flame in order to calculate the sound power emitted by the flame. Sound intensity was measured in a half-hemisphere by pressure-pressure-probes in order to record the total sound power of the direct combustion noise emitted by the unconfined flame. The goal of this study was to compare the measured sound power exhibited by the flame with the sound power predicted due to fluctuations of density within the flame. By using a siren to generate linear excitation, it was possible to qualitatively predict combustion noise with good agreement in trend. A quantitative comparison between both measurement techniques showed a deviation of a factor of six.

NOMENCLATURE

A_{meas}	[m^2]	cross-sectional area of the laser vibrometer beam
A_{surf}	[m^2]	surface area of microphone hemisphere
c_0	[m/s]	speed of sound
f	[Hz]	frequency
FFT		fast Fourier transform
G	[m3/kg]	Gladstone-Dale constant
I_r	[W/m^2]	radial component of sound intensity
Im		Imaginary part
k	[mm/s/V]	vibrometer calibration constant
LIV		laser interferometric vibrometry
lat		latitudinal coordinate
lng		longitudinal coordinate
MP		measurement point
natural spectrum		spectrum of flame without excitation
P_{far}, P	[W]	sound power
pp-probe		pressure-pressure probe
p’	[Pa]	sound Pressure
PPM det		detached perfectly premixed
r	[m]	radial distance of observer
r_0	[m]	radius of flame
t	[s]	time
TPM att		attached technically premixed
TPM det		detached technically premixed
U	[V]	voltage
v_r	[m/s]	radial component of particle velocity
V_{Fl}	[m^3]	volume of the flame
Δr	[m]	Distance between microphones of pp-probe
ρ_0	[kg/m^3]	mean density outside of the flame
ρ'_T	[kg/m^3]	density fluctuation within flame
ρ’(r)	[kg/m^3]	density fluctuation at radius of observer
ζ	[m]	length of laser vibrometer beam

INTRODUCTION

Combustion generated noise has been a topic for many years in industrial applications where reacting flows are predominantly turbulent. Especially the prediction, and consequently the reduction of correlated and stochastic sound radiation of flames has been investigated intensively [1, 2]. Early theories as well as experimental validations suggest that the far field sound pressure is proportional to fluctuations of heat release within the flame [3]. For measurability, many publications supported the use of the time derivative of OH*-Chemiluminescence [4]. However, the density distribution within the flame had to be assumed. Progress in combustion noise theory made it possible to predict sound emission directly as a function of heat release without the need of the mean density field [5], but it remains a difficult task to acquire the heat release acurately. Alternatively, early work [6] suggested the use the density fluctuations within the flame ρ'_T in order to estimate density fluctuations in the far field ρ' and consequently combustion noise:

$$\rho'(r) = \frac{1}{4\pi c_0^2 r}\frac{\partial^2}{\partial t^2}\int_V \rho'_T\left(r_0, t - \frac{r}{c_0}\right) dV(r_0) \qquad (1)$$

with c_0 speed of sound, r radial distance of observer, volume V and radius r_0 of the flame. Since time resolved density fluctuations were difficult to measure, an adaption of the equation with application of OH*-chemiluminescence estimating the mean density within the flame was often preferred [2], Recent development and experimental work enabled accurate measurements of time resolved line-of-sight and local density fluctuations in turbulent jets [7, 8] and in laminar [9] and turbulent flames [10, 11]. Therefore, it is now possible to prove Strahle's assumption directly. For the research presented herein, a novel technique recording the time derivative of the density fluctuation was used. The measurement device, a laser interferometric vibrometer (LIV), integrates along the laser beam path and scans the two dimensional field of the flame. In the standard application of vibrometers the motion of an object is measured. If that object is a fixed mirror the interferometer in the instrument measures the time derivative of the density fluctuations along the laser beam path.

THEORETICAL BACKGROUND

In the following paragraph the calculation of sound power from $\int_\zeta \partial\rho'_T/\partial t$ directly measured by LIV and from microphone measurements are presented. Comparing sound power has the advantage that this number does not dependent on the distance of the observer (microphone) and it is easier to measure if the far field condition is not met [12]. It has the same significance as comparing density fluctuations since in the far field sound power is a direct function of the density fluctuation. Flames have a low pass characteristic and in a laboratory environment the far field condition for low frequencies is usually not fulfilled. Therefore, it is more convenient to calculate and compare sound power, which is not a function of the radial distance to the flame.

Prediction of Sound Power from $\int_\zeta \partial\rho'_T/\partial t$

In the far field where sound pressure p' and particle velocity are in phase sound power P_{far} can be calculated from density fluctuations as follows.

$$P_{far} = 4\pi r^2 \frac{p'(r)^2}{\rho_0 c_0} = 4\pi r^2 \frac{(c_0^2\rho'(r))^2}{\rho_0 c_0} \qquad (2)$$

Here, a sphere is defined as detection surface. Combining Equation 1 and Equation 2 results in the sound power as a function of density fluctuations:

$$P_{far} = \frac{1}{4\pi\rho_0 c_0}\left(\frac{\partial^2}{\partial t^2}\int_{V_{Fl}} \rho'_T\left(r_0, t - \frac{r}{c_0}\right) dV(r_0)\right)^2 \qquad (3)$$

After performing a fast Fourier transform (FFT) - now in the frequency domain - the time derivative of a variable is simply the variable times the angular frequency with a time lag of pi/2 :

$$FFT\left(\frac{\partial\rho'_T}{\partial t}\right) = 2\pi f * FFT(\rho'_T, angle - 90°) \qquad (4)$$

Now, in frequency domain, the acoustic power in the far field $P_{far(f)}$ can be calculated for each frequency f from Equation 3.

$$\mathrm{P_{far}(f)} = \frac{1}{4\pi\rho_0 c_0}\left((2\pi f)(2\pi f)\int_{V_{Fl}} \rho'_T(\mathrm{phase} - 180°)\left(r_0, t - \frac{r}{c_0}, f\right)\right)^2 \qquad (5)$$

The integral density fluctuation over the flame volume $\int_{V_{Fl}} \rho'_T$ is equal to the sum of all fluctuations in the vibrometer grid, when the density fluctuations outside the flame are low compared to the ones within the flame. That this is the case, has been shown by [13].

$$(2\pi f)(2\pi f)\int_{V_{Fl}} \rho'_T(\mathrm{phase} - 180°)\left(r_0, t - \frac{r}{c_0}, f\right) = (2\pi f)\sum_{MP=1}^{n}\frac{4}{\pi}A_{meas}\int_\zeta \frac{\partial\rho'_T}{\partial t}(\mathrm{phase} - 90°)\left(r_0, t - \frac{r}{c_0}, f\right) \qquad (6)$$

with A_{meas}, the cross-sectional area of the laser vibrometer beam and ζ the measurement length of the vibrometers laser beam between optics and mirror. The factor $4/\pi$ corrects for a circular laser beam in a rectangular measurement grid. In this grid, the fluctuations outside of the circular beam cross-section would otherwise not be accounted for.

Combining Equation 5 and 6 yields the total sound power as the sum over all frequencies:

$$\sum_f P_{far}(f) = \sum_f \frac{1}{4\pi\rho_0 c_0}\left(2\pi f \sum_{MP=1}^{n} \frac{4}{\pi} A_{meas} \int_\zeta \frac{\partial \rho'_T}{\partial t}(phase - 90°)\left(r_0, t - \frac{r}{c_0}\right)\right)^2 \quad (7)$$

Equation 7 holds true if the flame diameter is small compared to the wavelength and distance to the observer. Then the space distribution of heat release can be neglected [6]. This is the case in our setup. If the flame diameter would be large, the spatial distribution of coherent heat release could not be neglected anymore. Extinction and amplification of pressure waves from local heat release (density) fluctuations would depend on the position of the source within the flame.

Calculation of Sound Power from PP-Probe

In the near field where sound pressure p' and the radial component of the particle velocity v_r are not in phase, sound power can be calculated via the radial component of sound intensity I_r which is perpendicular to the surface of the hemisphere A_{surf}:

$$P = \int_A I_r dA_{surf} = \int_A p' v_r dA_{surf} \quad (8)$$

Pressure is far easier to measure than particle velocity, therefore, the Euler equation is often used to estimate the particle velocity [12]:

$$\frac{\partial v_r}{\partial t} = -\frac{1}{\rho_0}\frac{\partial p}{\partial r} \quad (9)$$

The velocity along one dimension can then be expressed as a function of the pressure at two different positions:

$$v_r = -\frac{1}{\rho_0}\int_t \frac{p_{r+\Delta r} - p_r}{\Delta r} dt \quad (10)$$

As a consequence, the sound intensity in radial direction can be calculated by

$$I_r = p v_r = -\frac{p_{r+\Delta r} + p_r}{2}\frac{1}{\rho_0}\int_t \frac{p_{r+\Delta r} - p_r}{\Delta r} dt \quad (11)$$

For spectral analysis sound intensity can be expressed as a function of the imaginary part of the cross product of the complex pressures:

$$\vec{I}(f) = p\vec{v} = -\frac{1}{\rho_0 2\pi f \Delta r} Im(FFT(p_{r+\Delta r)} \times FFT(p_{r)}) \quad (12)$$

The cross product in the frequency domain can then be calculated by complex conjugated multiplication:

$$FFT(p_{r+\Delta r)} \times FFT(p_{r)} = FFT(p_{r+\Delta r)} * FFT(p_{r)}^* \quad (13)$$

EXPERIMENTAL SETUP

Test Rig

For the investigations presented in this paper, a variable geometry burner was used and the flow was excited with a siren which was mounted into the axial air-feed-line. The working principle of the burner has been documented in detail [14], the flow-field and characteristics of the - for rotational symmetry adapted - design have been published recently [15]. The siren was equipped with a sonic nozzle which had 1 mm in diameter, followed by a rotating cogwheel, blocking the crossectional area of the nozzle by 100%. Details about the siren can be found in [16]. In Figure 1 the burner is shown with the standard configuration - technically premixed (TPM) - to the left and the reference configuration - perfectly premixed (PPM) - to the right of the setup.

In the TPM configuration, the combustor is fed by fuel (a) tangential air (b), and axial air (c). The axial air is forced through a stratifier in order to ensure purely axial flow. In

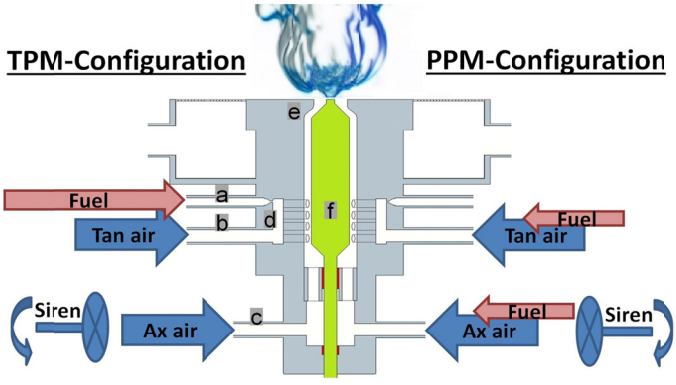

FIGURE 1: THE EXPERIMENTAL SETUP WITH THE TPM CONFIGURATION TO THE LEFT AND THE PPM CONFIGURATION TO THE RIGHT

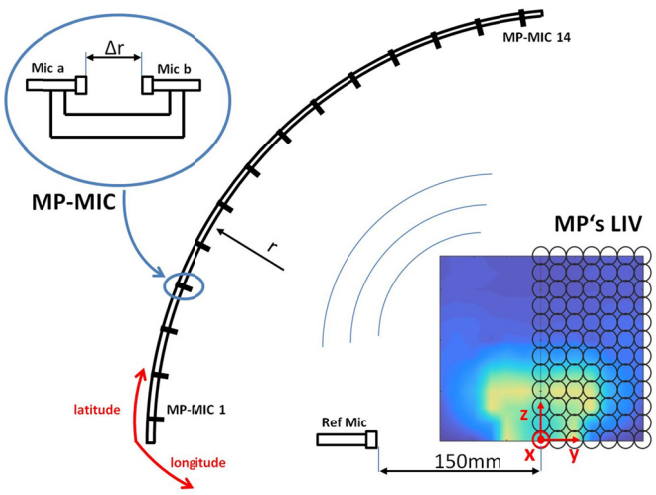

FIGURE 2: PP-PROBE-SETUP WITH TWO MICROPHONES (TOP LEFT), PP-PROBE MP'S ONE TO FOURTEEN IN ARCH-CONFIGURATION AND LONGITUDINAL TRAVERSING DIRECTION (MIDDLE) AND 2D-MEASUREMENT GRID OF LIV (BOTTOM-RIGHT).

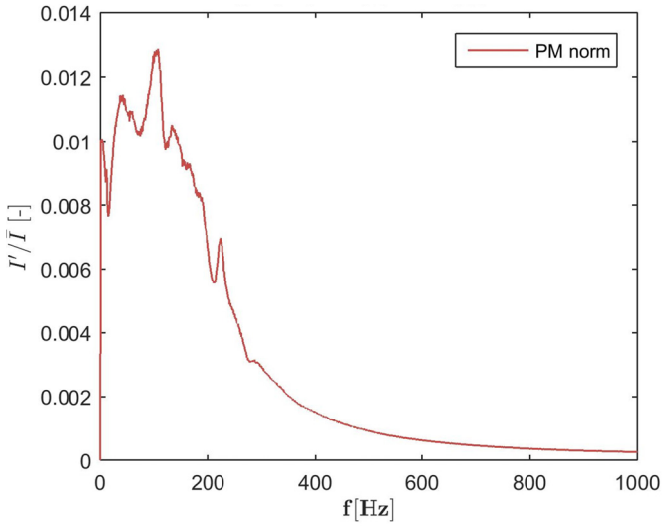

FIGURE 3: NATURAL OH*-CHEMILUMINESCENSE SPECTRUM OF PPM DET.

contrast to this the tangential air passes the outer mixing chamber (d) and from there, enters the plenum through 32 cylindrical bores aligned tangentially and symmetrically around the burner axis. Methane is injected into the tangential air in the outer chamber. The siren modulates the axial gas flow only.

In case of perfect mixing, the methane was injected into the air supply far upstream before tangential and axial air split. The movable center cone (f) of the burner was set to 1 mm above the exit in order to constrict the flow through the burner exit nozzle (e) and consequently ensure correct momentum for the point of operation. Mass flow was measured using caloric mass flow meters of the EL-FLOW series from Bronkhorst, Netherlands, with an accuracy of 0.6 % FSC. The test rig was set up in a thermoacoustic laboratory within a 3x3x2.5m3 box with two layers of low reflective curtains and a sound absorbing ceiling. The specific mass flows of the points of operation can be found in Table 1. The simplified swirl number was measured according to [17], neglecting the pressure term, using a burner exit radius of 8 mm averaging over a height of z=8.5 mm to z=17 mm which is 0.5 times and 1 time the burner exit diameter respectively.

For this investigation three points of operation were examined. In the technically premixed setup two flame shapes are stable. Generally, the flame is attached to the center rod of the burner. Once the flame detaches the flame stays detached in a stable way. In the perfectly premixed setup the flame was detached all the time - the flame cannot anchor at the bluff body of the burner-center-rod.

MEASURING TECHNIQUES

Microphone Array

For the acoustic measurements, a custom built microphone array, with 14 measurement positions aligned in an arch of one meter radius, was built (Figure 2). At those 14 measurement points in latitudinal direction, acquisition was performed simultaneously. The setup covered 90° in 6° steps of the downstream area of the flame. In longitudinal direction (around the positive z-axis), the burner was rotated in 6°steps to cover a semicircle. At each of the measurement positions two microphones where set up facing each other. With this configuration, also known as pp-probe [18], acoustic pressure was measured directly and particle velocity was derived. From that configuration the sound intensity can be calculated, as well as, the total sound power without a need to fulfill the far-field assumption.

The distance between two opposing microphones was 56 mm. This provides accurate measurements for the frequency spectrum between 50 and 1000 Hz, which covers the spectrum of the flame investigated [18]. Additionally, two microphones were rotated with the burner in order to provide a reference signal. They were used to normalize the sound intensity signal

Table 1: Flow properties

Axial air [g/s]	Tangential air [g/s]	Fuel [g/s]	Swirl Number [-]
0.422	0.397	0.0683	0.54

in order to account for slight variations in the point of operation of the burner. The photomultiplier (PMM01, Thorlabs Inc., Newton, New Jersey, USA with OH* filter 310 nm CWL,

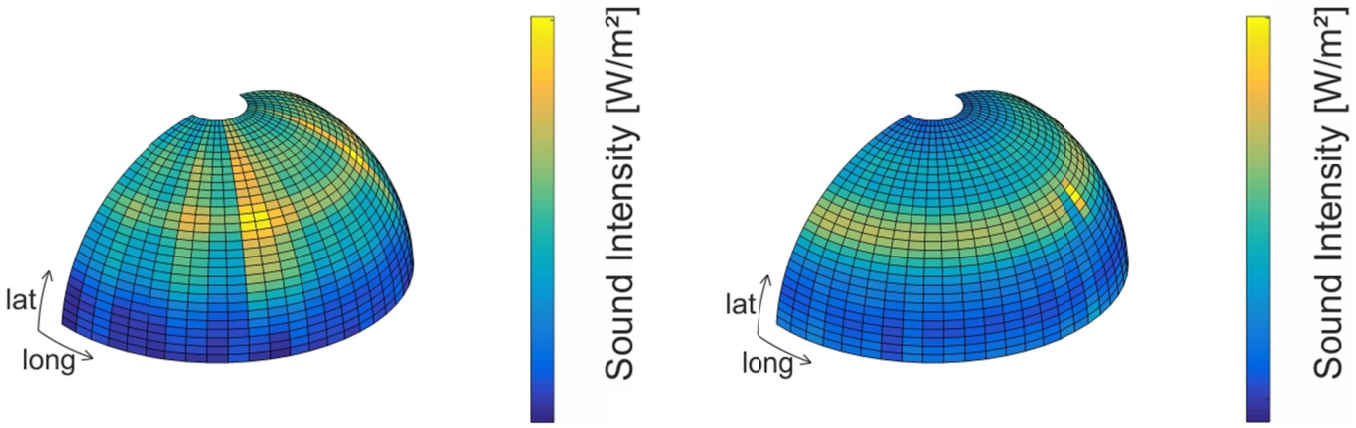

FIGURE 4: SOUND INTENSITY DISTRIBUTION BEFORE (LEFT) AND AFTER (RIGHT) NORMALISATION BY THE REFERENCE MICROPHOHNE.

FWHM 10 $\pm$2 nm Bandwidth, Edmund Optics, Barrington, NJ, USA) and the siren signal were acquired as well. This gives a total of 32 channels which were recorded with a PXI-module and Labview 8.6 software, both from National Instruments, Austin, Texas, USA. The sample rate of was 100 kilo samples per second.

Laser Interferometric Vibrometry

Here, laser interferometric vibrometry (LIV) detects the time derivative of line-of-sight integrated density fluctuations in a gas by interferometric principles [19, 7, 8, 9, 11]. Using a Polytec laser vibrometer (interferometer head OFV-353, velocity decoder OFV-3001, calibration factor 5mm/s/V, 200 kHz bandwidth, no filters, Polytec, Waldbronn, Germany) the measured voltage (U) is linked to the derivative of the density fluctuation by the Gladstone-Dale constant (G) and the calibration factor (k). G and k were set to 2.59e-4 m^3/kg and 5 mm/s respectively for all points of operation:

$$\int_{\zeta} \frac{\partial \rho'_T}{\partial t}(A_{meas}, \zeta, t) d\zeta = \frac{k}{2G} U(t) \qquad (14)$$

In velocity mode the output voltage U(t) is linked to the line of sight integrated derivative of the density fluctuation in the flame $d\rho'_T/dt$ per measurement area A. A factor of two is due to the laser beam passing the cylindrical measurement volume twice. The beam diameter was set to 5mm. The field was scanned from z = 5 mm to 60 mm and from y = 0 to 30 mm with 5 mm increment (Figure 2). The beam direction with integration length ζ is parallel to y coordinate.

Processing

Evaluation of both data sets, LIV and microphone, was performed in Matlab 2015a using Welch's periodogram [20] and the analogous cross product function with a sample length of 100,000. The built in flattop window was applied for all single frequency investigations, in order to face the scalloping loss of FFT. For the spectrum-integrated data, a rectangular window was used.

Schlieren

For visualization of density gradients in space, a schlieren technique [21] was applied. The same setup as in [15] was used, but now the camera was triggered with the siren signal, and one hundred images were acquired and averaged.

RESULTS AND DISCUSSION

Below, the acoustic behavior of the flame in the three different configurations is discussed. In a first step, the natural sound spectrum (no siren) and the radiation behavior will be analyzed. Then, by excitation with a siren, the linear behavior of the flame at a single frequency is discussed. A quantitative benchmark with the sound power, calculated from heat release using Strahle's Equation 1, should deliver a similar result. This is only possible by a high enough signal to noise ratio, necessary to ensure comparability between the two different measurement techniques, and is achieved by linear excitation with a siren. Finally, the schlieren technique is used to discuss different trends of noise levels between points of operation for the natural spectrum and mono frequent excitation.

Acoustics

Since the typical hydrocarbon flame acts as a low pass filter, the spectrum of the heat release is usually characterized first by a rapid increase of amplitude with increasing frequency that tops out on a smooth peak and is followed by a gentle slope towards higher frequencies. This typical behavior is shown in the OH*-chemiluminescence image in Figure 3.

In a first step, **the natural spectra** of the flames were recorded. In Figure 4 the sound intensity calculated from

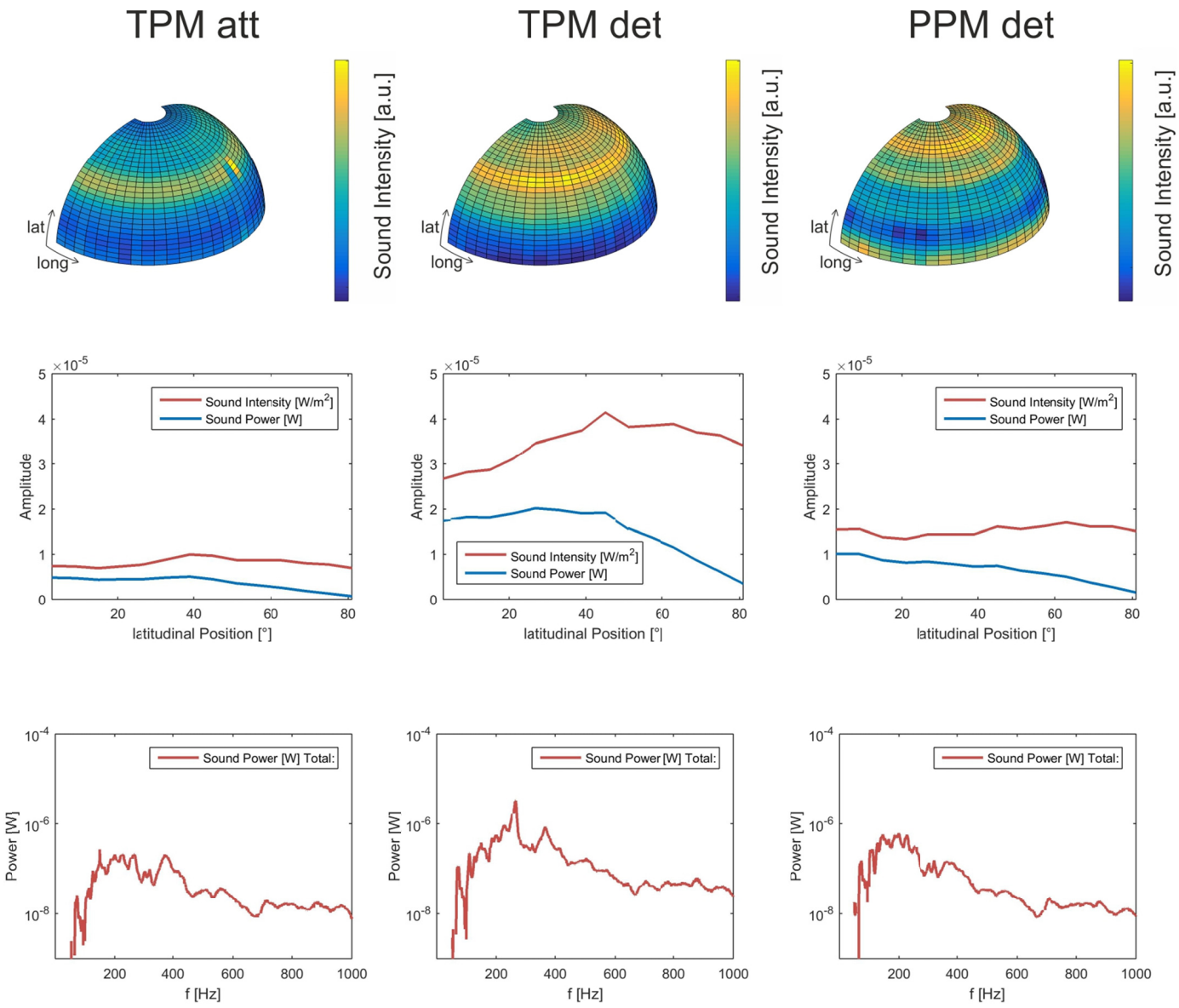

FIGURE 5: SOUND INTENSITY DISTRIBUTION (TOP), INTENSITY AND POWER ALONG LATITUDINAL POSITIONS (MIDDLE) AND TOTAL SOUND POWER SPECRUM (BOTTOM) FOR ALL THREE POINTS OF OPERATION.

Equation 12 integrated over all frequencies is plotted in half a hemisphere, as a function of longitudinal and latitudinal coordinates. The latitudinal measurement points were acquired simultaneaously, while the longitudinal measurement points were acquired one after the other, by rotating the burner. Before normalization (Figure 4 left), two trends are obvious. Firstly, the sequential measurement method introduces a fluctuation of sound intensity (longitudinal direction). Secondly, sound intensity also depends on latitudinal position. In order to interpret the result properly, the measurement of half the hemisphere was normalized by a reference microphone, which was traversed with the burner. The pressure signals used for the calculation were normalized for each frequency in the spectrum and each latitudinal (lat) and longitudinal (long) position individually according to:

$$p'^2{}_{norm}(lng, lat, f) = \frac{p'^2(lng, lat, f)}{p'^2{}_{ref}(lng, f)} * \overline{p'^2{}_{ref}(f)}^{lng} \qquad (15)$$

with the normalized pressure signal p'_{norm} calculated from the original signal p' and the reference signal p'_{ref}. This linear normalization of the square of the pressure is equivalent to normalization of the sound power. This simple correction results in a nearly perfect rotationally symmetric distribution of sound intensity (Figure 4 left) and confirms the assumption of an axis symmetric flame [22]. Consequently it was not

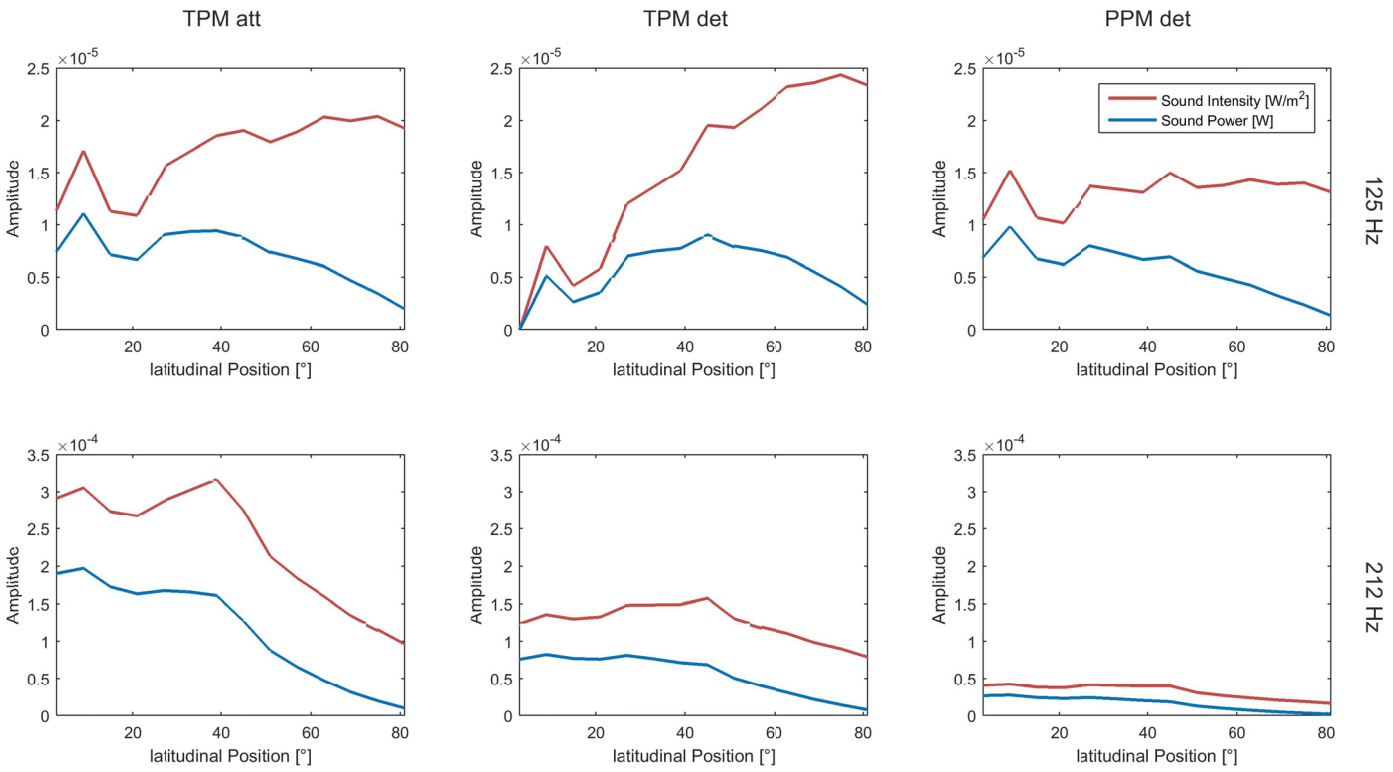

FIGURE 6: SOUND INTENSITY (TOP) AND POWER (BOTTOM) FOR LINEAR EXCITATION AT 125 HZ AND 212 HZ FOR ALL THREE POINTS OF OPERATION.

necessary to measure the whole field of half a hemisphere. To double-check the results and due to the short acquisition time of 20 seconds per measurement point this task was performed, since small variations in burner operation are inevitable. Therefore, for all results presented in this work, the 30 longitudinal measurement points were averaged in order to provide repeatable results.

The sound intensities for all three points of operation normalized by the reference microphone are presented in Figure 5 (top). Averaging over longitudinal measurement points gives sound intensity and derived from that, sound power as a function of latitude (Figure 5 middle). Finally a spectrum of total sound power / Hz is shown (Figure 5 bottom).

For all points of operation, a weak directionality can be found, as literature has suggested [23]. The attached TPM flame shows its highest amplitude of sound intensity at 45° downstream, falling off in amplitude towards higher as well as lower angles. The overall sound power is lowest for this configuration. Similar results can be found for the detached TPM configuration, the peak amplitude is located at the same latitude of about 45°, but now sound intensity stays high towards higher frequencies. The overall sound power is highest for this configuration. Finally, the detached PPM case shows a local peak sound intensity at 45°, but now it is topped by the noise in downstream direction. The overall noise level is in-between the noise of the other two points of operation.

The reason that the attached flame was the quietest one can be found in the flame stabilization process. The flame is anchored in the wake of the center cone of the burner which is a stable point in space. This makes the flame less receptive to small turbulent fluctuations from upstream. In contrast to this - in the detached configuration - the flame is stabilized solely by the swirl induced recirculation zone, which generally makes the flame much more receptive to flow field disturbances such as vortex shedding and other fluctuations. In the frequency spectra of the sound power (Figure 5 bottom), this can be seen as well.

The detached TPM case shows a mono-frequent effect at around 250 Hz, which has been identified in previous work as vortex shedding at the burner exit [24]. The vortices follow the conical jet of the swirl outwards and interact with the recirculated reactants. The angular direction of the swirl jet roughly meets the latitudinal angle of highest amplitude in sound intensity distribution. PPM det and TPM att have a less mono-frequent pattern in spectrum, explaining a lower overall sound emission. All three operation points have in common that in their spectra, hardly any combustion noise is present above 500 Hz. This fact is not surprising when comparing with the OH* emission in Figure 3. Integrating over the whole spectrum of sound power gives a total sound power of 5.06*10-5 W, 2.1*10-4 W and 9.34*10-5 W for TPM att, TPM det, and PPM det respectively. With a thermal power of the flame of 3.4 kW this gives thermal efficiencies of 1.5*10-8, 0.6*10-7 and

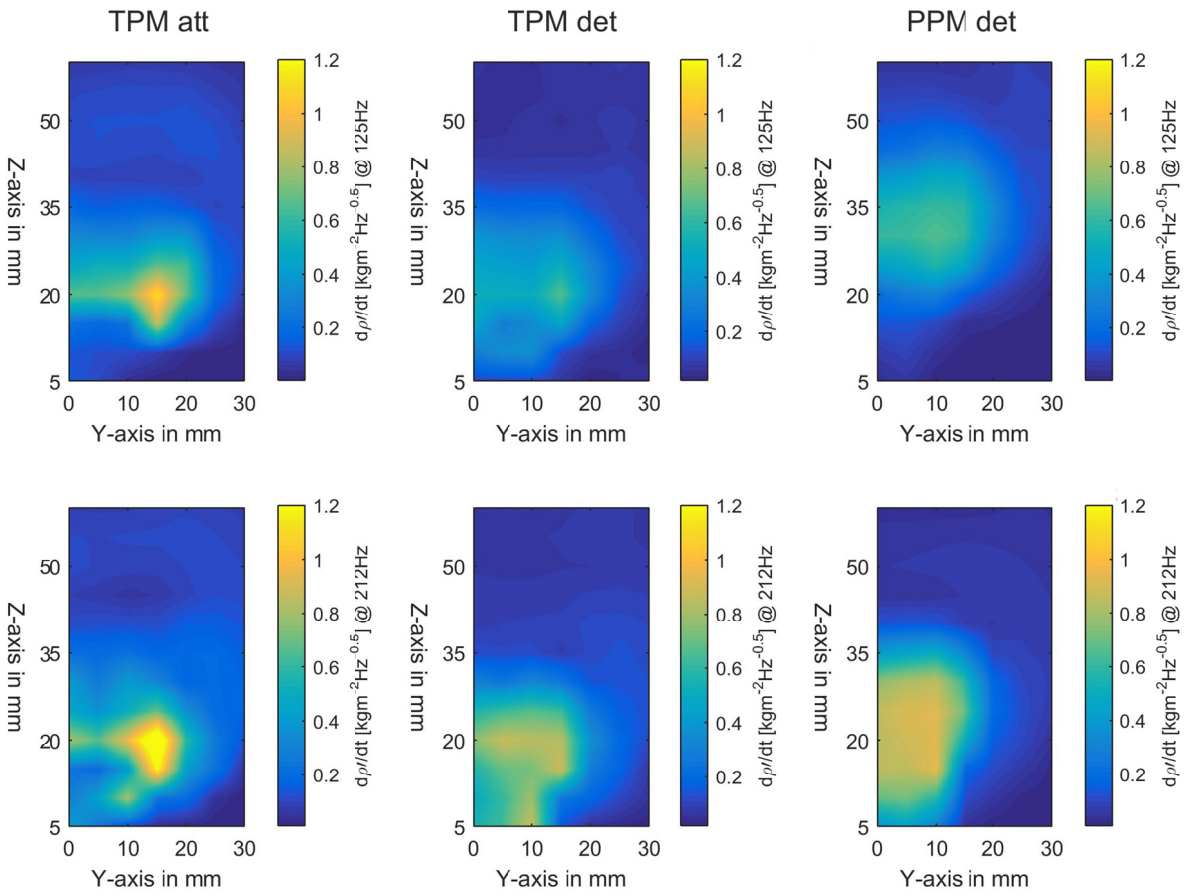

FIGURE 7: TIME DERIVATIVE OF LINE-OF-SIGHT-INTEGRATED DENSITY FLUCTUATIONS MEASURED BY LIV FOR 125 HZ AND 212 HZ EXCITATION. THE PLOTTED VALUE IS THE AMPLITUDE RESULTING FROM FFT.

2.8*10-8. This lies in the range of 10-8 to 10-7 which is consistent with other research [25, 23].

In a second step, the flame was **excited by a siren**. All parameters were kept constant, only the excitation frequency was altered. Sound intensities were averaged for half the hemisphere. Power and sound intensity can be found in Figure 6 for 125 Hz and 212 Hz. The trend for 125 Hz along the height is very similar to the natural spectrum discussed above. At both TPM cases the noise level increases with latitude. Except now for TPM det the sound intensity is close to zero at the bottom of the microphone array. In contrast to this, the excitation at 212 Hz shows an entirely different behavior. Now the amplitude is high at low measurement positions and gradually decreases with increasing latitude.

Sound Prediction by LIV

The time derivative of density fluctuations were measured by means of LIV. With some assumptions, this quantity is proportional to the heat release rate fluctuations in the flame [9, 11]. In Figure 7 the amplitude distributions for siren excitation at 125 Hz (top) and at 212 Hz (bottom) are shown. For all points of operation, the total fluctuation of density stretches widely in radial as well as in axial direction. For PPM the fluctuations are further downstream in comparison to the technically premixed flame. This can be explained by an increased axial momentum at perfect mixing, where half of the fuel is injected into the axial flow. In contrast to this, in case of technical mixing, the entire fuel is injected tangentially. Looking at the excitation at 125 Hz it is obvious that the major fluctuations are within the core of the flame, which is at around z = 20 mm for the TPM cases and at around z = 30 mm for the PPM case. In contrast to this, at 212 Hz the major fluctuations of the detached configurations are smaller in amplitude. The flame seems to be strongly excited by incoming perturbations at this frequency. Especially the detached flames change the position of main oscillations. Comparing the density fluctuations at 212 Hz with the sound power measured by the microphone array as shown in Figure 6, one could explain the trend of the flame to radiate more in horizontal direction (side-wise) at this frequency. Generally a greater surface of heat release fluctuations will lead to higher noise radiation as long as those zones are correlated in phase.

For the comparison of sound power calculated from the density fluctuations within the flame and the sound power

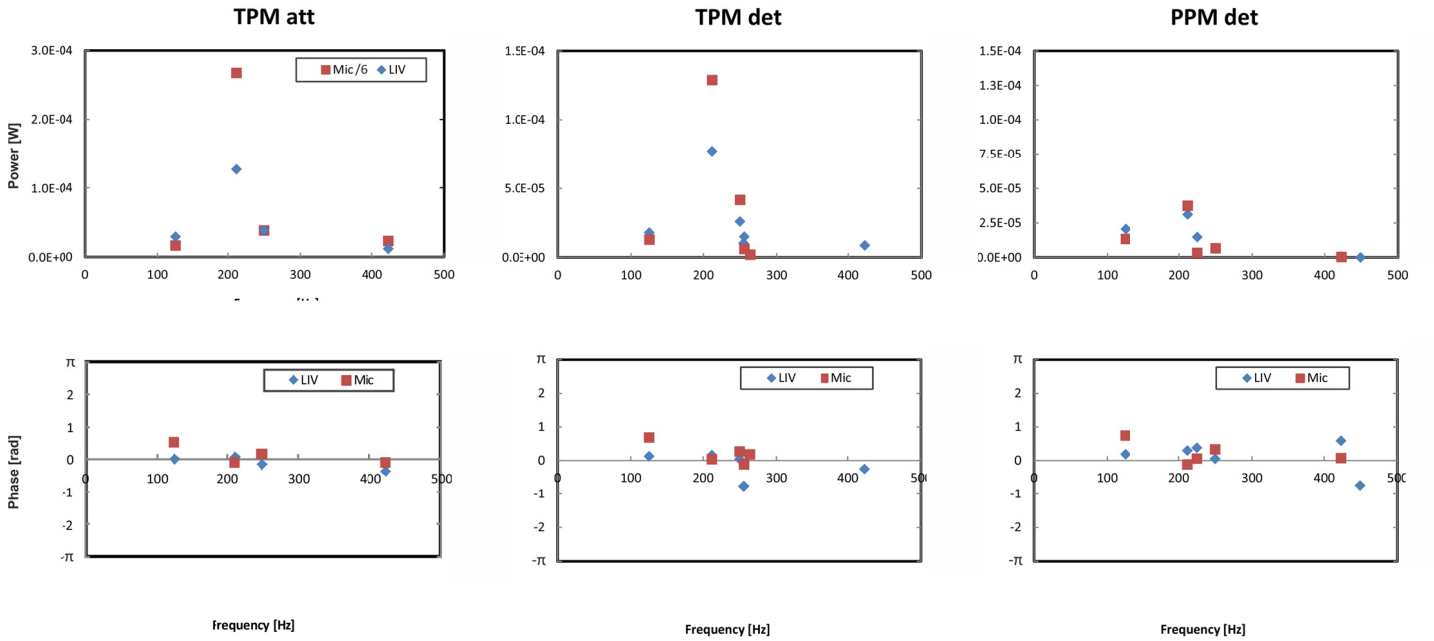

FIGURE 8: AMPLITUDE AND PHASE OF SOUND POWER MEASURED BY MICROPHONES AND LIV, WITH PM AS REFERENCE FOR THREE POINTS OF OPERATION, EXCITATION BY SIREN.

measured by the microphone array, linear excitation by a siren was done. The amplitude of sound pressure measured by microphones and prognosed due to the heat release from LIV are in a comparable range. For the microphone measurements sound power lies between 2e-3 mW for the PPM flame at 423 Hz and 1.6 mW for the attached TPM flame at 212 Hz.

For the same measurement points vibrometry prognosed a sound power level of 0.7e-3 mW and 0.13 mW respectively. This is less than one order of magnitude in difference. The comparison of trends over frequencies is shown in Figure 8. For the sake of visualization in Figure 8, the microphone results were divided by a factor of six. This makes it possible to see the matching trend over frequencies for both measurement techniques (Figure 8 top). For both, the attached TPM flame (Figure 8 left) shows highest fluctuations over the whole band of frequencies, followed by TPM det (Figure 8 middle), which is consistently quieter. Finally, the PPM det flame (Figure 8 right) is the quietest one throughout the spectrum. Considering the individual frequencies, similar trends can be found for all points of operation. At 125 Hz low sound pressure is measured, with good consistency of both measurement techniques for all points of operation. Moving on to 212 Hz the acoustic sound due to combustion is highest, and at the same time the prediction of sound by LIV slightly underestimates the actual

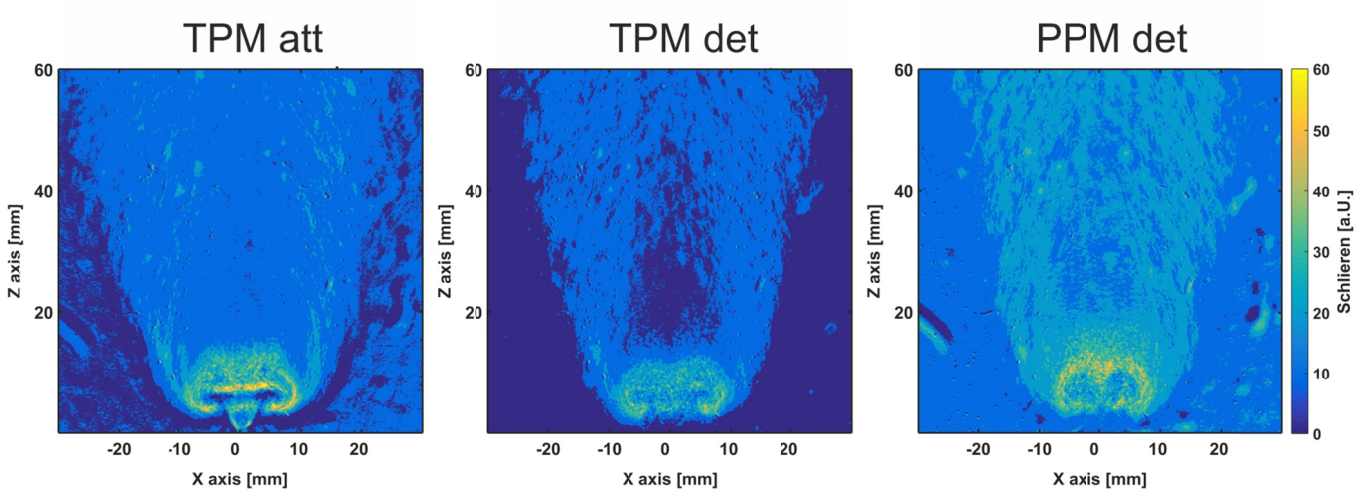

FIGURE 9: DENSITY GRADIENTS IN SPACE OF ALL POINTS OF OPERATION AT 212 HZ AND 315° PHASE ANGLE VISUALIZED USING SCHLIEREN TECHNIQUE.

sound power. From higher frequencies onward, the consistency of trends for both techniques is again very good.

For linear excitation, the phase of the sound power derived from LIV and the microphone array is plotted in Figure 8 (bottom). Measurements show that for all frequencies tested the phase of the LIV is very close to the photomultiplier signal. A low deviation of no more than 30 degrees (mostly below 10 degrees) is expected, since both techniques represent the heat release of the flame. In order to compare the phase of the microphone with the phase of heat release recorded by LIV, firstly, one has to account for the time delay, the acoustic wave needs for the distance between the flame and the microphones. Secondly, the vibrometer signal is proportional to $\partial\rho/\partial t$, but the resulting sound is proportional to the second time derivative of density. 90° phase shift have to be accounted for when the time derivative of a signal is calculated in the frequency domain. Therefore, the phase of the acoustics was corrected by adding a phase shift which is a function of the distance between flame and measurement position as well as the frequency. Then $\pi/2$ was subtracted to correct for the time derivative in frequency domain.

Analysis of Specific Sound Levels

When comparing the natural spectrum and the amplitudes of linear excitation for the sound power measured by microphones, it can be found that the PPM detached flame is consistently quieter than the TPM det flame. However, the TPM att case is the quietest one for the natural spectrum but with excitation, all of a sudden, it becomes the noisiest flame. The reason for the natural spectrum to be of lowest amplitude has been identified to lie in the stabilization process of the anchored flame. But then, with siren excitation, the fluctuations of heat release get so violent that the flame anchoring region behind the bluff body is heavily disrupted. In Figure 9 left density gradients in space at one frequency and one phase angle are shown. The surface of the attached flame is heavily disrupted. At the end of the flame cone vortex an induced flame roll up is observed. This process enlarges the flame surface and coherent fluctuations in heat and consequently in noise can be observed. The attached V-cone flame almost acts like a rubber band, trying to keep the vortex attached to the flame, and then suddenly snaps back. In comparison to this, the other points of operation are purely dynamically stabilized. Therefore, those flames can, within limits, travel up and downstream of the flow, dampening the process. Vortex rollup, which introduces shear stress in the flow, is more suppressed by this flame motion. The vortex rollup in the flame can still be found in the detached flames (Figure 9 middle and right), but the density gradients are more smeared.

CONCLUSION

Strahle postulated that the sound of a flame in the far field is a function of density fluctuations within the flame. The focus of this study was to prove Strahle's assumption by comparison between the predicted noise measured with LIV and a microphone array. In the first part, the acoustic field of the flame was analyzed. Normalization by the reference microphone corrected for sub-Hz frequency fluctuations during operation, results in an almost perfectly symmetrical sound field. In latitudinal direction, a slight dependency on angle was found as detected by other authors [23]. Overall sound power is in agreement with experience of former work as well. For the level of noise, the stabilization process was found to be the dominant factor. For siren excitation, the angular variation of sound intensity was traced back to the distribution of combustion fluctuations, which were particularly intense at the root of the flame.

Considering sound prediction by heat release fluctuations qualitatively, both measurement techniques lie in the same order of magnitude. In this study LIV underestimated the actual sound level by a factor of six. A very good agreement in trend over the range of investigated frequencies was shown. Some factors of influence lie within the equation of sound power due to density fluctuations. First, the assumption of a monopole, second, in the equation the diameter of the laser beam raised to the fourth is considered. Therefore, it is critical to accurately determine the diameter when the system is set up.

Finally, the behavior of the TPM att was explained by means of the schlieren technique. This operation point initially was the quietest. However, once excited by the siren, it consistently had the highest amplitude.

This leads to the final conclusion, that it is possible to predict combustion noise qualitatively due to density gradients within the flame. On the basis of direct physical quantities a comparison of both techniques revealed a deviation by a factor of six.

ACKNOWLEDGEMENT

This research was funded by the Austrian Science Fund (FWF) within grant FWF-24096-N24 "Interferometric Detection of Thermoacoustic Oscillations in Flames".

References

[1] W. C. Strahle, "Combustion noise," *Progress in Energy and Combustion Science,* vol. 4, no. 3, pp. 157-176, 1978.

[2] T. Schuller, D. Durox and S. Candel, "Dynamics of and Noise Radiated by a Perturbed Impinging Premixed Jet Flame," *Combustion and Flame,* vol. 128, pp. 88-110, 2002.

[3] R. B. Price, I. R. Huerle and T. M. Sudgen, "Optical studies of generation of noise in turbulent fames," *Twelfth Symposium (International) on Combustion,* 1969.

[4] I. R. Huerle, R. B. Price, T. M. Sudgen and A. Thomas, "Sound emission from open turbulent flames," *Proc. R. Soc. A,,* 1968.

[5] A. P. Dowling and Y. Mahmoudi, "Combustion noise," *Proceedings of the Combustion Institute,* vol. 35, no. 1, pp.

65-100, 2015.

[6] W. C. Strahle, "On combustion generated noise," *Journal of Fluid Mechanics,* vol. 49, no. 02, pp. 399-414, 1971.

[7] B. Hampel and J. Woisetschläger, "Frequency- and space-resolved measurement of local density fluctuations in air by laser vibrometry," *Measurement Science and Technology,* vol. 17, pp. 2835-2842, 2006.

[8] N. Mayrhofer and J. Woisetschlaeger, "Frequency analysis of turbulent compressible flows by laser vibrometry," *Experiments in Fluids,* vol. 21, pp. 153-161, 2001.

[9] T. Leitgeb, T. Schuller, D. Durox, F. Giuliani, S. Köberl and J. Woisetschläger, "Interferometric determination of heat release rate in a pulsated flame," *Combustion and Flame,* vol. 160, no. 3, pp. 589-600, 2013.

[10] J. Li, D. Durox, F. Richecoeur and T. Schuller, "Analysis of chemiluminescence, density and heat release rate fluctuations in acoustically perturbed laminar premixed flames," *Combustion and Flame,* vol. 162, no. 10, pp. 3934-3945, 2015.

[11] J. Peterleithner, N. V. Stadlmair, J. Woisetschläger and T. Sattelmayer, "Analysis of measured flame transfer functions with locally resolved density fluctuation and OH-Chemiluminescence Data," *Journal of Engineering for Gas Turbines and Power,* vol. 138, no. 3, 2016.

[12] M. Möser, Engineering Acoustics, Vienna, New York, Heidelberg, 2014, p. 552.

[13] A. P. Dowling and A. S. Morgans, "Feedback Control of Combustion Oscillations," *Annu. Rev. Fluid Mech.,* vol. 37, pp. 151-182, 2005.

[14] F. Giuliani, J. W. Woisetschläger and T. Leitgeb, "Design and validation of a burner with variable geometry for extended combustion range," in *Proceedings of the ASME Turbo Expo*, 2012.

[15] J. Peterleithner, F. Salcher and J. Woisetschläger, "Frequency resol ed interferometric detection of local density fluctuations in flames," *Proc. 17th International Symposium on Application of Laser Techniques to Fluid Mechanics, Lisbon,,* 2014.

[16] F. Giuliani, A. Lang, K. Johannes Gradl, P. Siebenhofer and J. Fritzer, "Air flow modulation for refined control of the combustion dynamics using a novel actuator," *Journal of Engineering for Gas Turbines and Power,* vol. 134, no. 2, 2012.

[17] S. Candel, D. Durox, T. Schuller, J. .. Bourgouin and J. P. Moeck, Dynamics of swirling flames, vol. 46, 2014, pp. 147-173.

[18] Brüel and Kjaer, *Sound intensity,* 1993.

[19] J. Peterleithner and J. Woisetschläger, "Laser vibrometry for combustion diagnostics in thermoacoustic research," *Technisches Messen,* vol. 82, no. 11, pp. 549-555, 2015.

[20] A. V. Oppenheim and R. W. Schafer, Digital signal processing, Englewood Cliffs, N.J.: Prentice-Hall., 1975.

[21] G. Settles, Schlieren and Shadowgraph Techniques, Springer, Wien Heidelberg New York, 2006.

[22] J. Peterleithner, A. Marn and J. Woisetschläger, "Interferometric In estigation of the thermo-acoustics in a swirl stabilized Methane flame," in *Proceedings of the ASME Turbo Expo*, 2015.

[23] T. J. B. Smith and J. K. Kilham, "Noise Generation by Open Turbulent Flames," *Journal of Acoustical Society of America,* vol. 35, no. 05, pp. 715-724, 1963.

[24] J. Peterleithner, R. Basso, F. Heitmeir, J. Woisetschläger, S. R., C. J. and A. Fischer, "COMPARISON OF FLAME TRANSFER FUNCTIONS ACQUIRED BY CHEMILUMINESCENCE AND DENSITY FLUCTUATION," in *Proc. ASME Turbo Expo*, 2016.

[25] J. Wäsle, A. Winkler and S. T., "Spatial Coherence of the Heat Release Fluctuations in Turbulent Jet and Swirl Flames," *Flow, Turbulence and Combustion,* vol. 75, pp. 29-50, 2005.

